CFD Letters

Journal homepage:
https://semarakilmu.com.my/journals/index.php/CFD_Letters/index
ISSN: 2180-1363

Stability Analysis of Unsteady Mixed Convection Flow Near the Stagnation Point with Buoyancy Effect

Nurul Amira Zainal[1, 2], Kohilavani Naganthran [3], Roslinda Nazar[1,*]

[1] Department of Mathematical Sciences, Faculty of Science and Technology, Universiti Kebangsaan Malaysia, 43600 Bangi, Selangor, Malaysia
[2] Fakulti Teknologi Kejuruteraan Mekanikal dan Pembuatan, Universiti Teknikal Malaysia Melaka, Hang Tuah Jaya, 76100 Durian Tunggal, Melaka, Malaysia
[3] Institute of Mathematical Sciences, Faculty of Science, Universiti Malaya, 50603 Kuala Lumpur, Malaysia

ARTICLE INFO

Article history:
Received 14 July 2022
Received in revised form 15 August 2022
Accepted 18 September 2022
Available online 1 May 2023

Keywords:
Unsteady flow; mixed convection; hybrid nanofluids; stability analysis

ABSTRACT

This numerical study investigates the behaviour of the unsteady mixed convection flow and heat transfer near the stagnation region past a vertical plate in Al_2O_3-Cu/H_2O hybrid nanofluids. By choosing an appropriate similarity transformation, an ordinary differential equations system is obtained, hence scrutinized via the bvp4c package embedded in the MATLAB program. The results show that as the nanoparticle volume fraction and unsteadiness parameter increase, the fluid's skin friction coefficient also increases. Also, an increase in the nanoparticle volume fraction and unsteadiness parameter has broadened the range of solutions hence, delayed the progress of boundary layer separation. In addition, the presence of the unsteadiness parameter provides a significant result in the thermal system. The first solution is declared stable by the stability analysis.

1. Introduction

Hybrid nanofluids, derived from the distribution of nanoparticles in conventional fluids, are a new class of highly prospective fluids for industrial applications. These fluids are made up of metallic or non-metallic particles to create the appropriate combination of hybrid nanofluids. Hybrid nanofluids have been used in various applications, including heat transmission [1, 2]. According to prior results, the heat transfer properties of ordinary fluid improve when nanoparticles are suspended in them, increasing the thermal conductivity [3]. However, choosing suitable nanoparticles is one of the most crucial components of maintaining a stable hybrid nanofluids composition. Further analysis of boundary layer flow and heat transfer with different governing parameters are available in refs. [4–7], while additional studies on various types of fluids may be found in Refs. [8–11].

Mixed convection flow has piqued the interest of scholars due to its importance in the manufacturing industries. Jamaludin *et al.,* [12] performed outstanding work on analysing mixed convection stagnation point flow with thermal radiation and heat source/sink effects. Neverth eless,

* *Corresponding author.*
E-mail address: rmn@ukm.edu.my (Roslinda Nazar)

https://doi.org/10.37934/cfdl.15.5.5464

the study mentioned above is about constant flows. In some cases, a change in the free stream velocity or the surface temperature might cause the flow to become unstable. Devi *et al.,* [13] used boundary layer approximations to investigate the buoyancy impact on the unsteady stagnation point flow over a vertical surface. In another investigation, Noor *et al.,* [14] discovered that the heat transfer performance improved in mixed convection stagnation point involving the unsteady three-dimensional flow. Recent studies of the heat transfer and boundary layer flow in hybrid nanofluid may be obtained in Refs. [15–18].

The current study intended to address a knowledge gap, specifically in the study of mixed convection flow with buoyancy impact. To our knowledge, no prior studies have examined the stability analysis of unsteady mixed convection flow near the stagnation point flow with buoyancy effect in their research framework. The buoyancy effects induce a longitudinal pressure gradient, which modifies the velocity and heat-transfer characteristics of the basic forced-convection flow. The construction of a new mathematical hybrid nanofluids model was a major contribution to this numerical investigation. This study also remarked on the appearance of multiple solutions, urging an analysis of solutions stability to test their reliability. This crucial contribution may help to improve industrial production since conditions under buoyancy effects are significant in practical interest.

2. Mathematical Model

We defined (x, y) as Cartesian coordinates at $y = 0$, the surface and surrounding temperature are denoted as $T_w(x,t)$ and T_∞, respectively, while the velocity is given by $u_e(x,t)$ at $t = 0$ as in Figure 1. Under the prior assumptions and boundary conditions, the problem formulation can be signified in Cartesian coordinates as follows [12,13]:

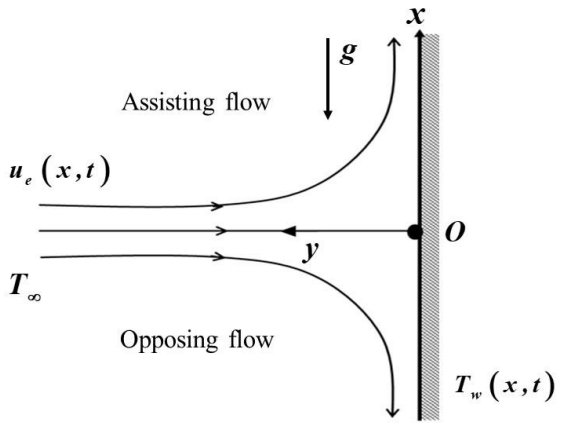

Fig. 1. Physical illustration and coordinate system

$$\frac{\partial u}{\partial x} + \frac{\partial v}{\partial y} = 0, \tag{1}$$

$$\frac{\partial u}{\partial t} + u\frac{\partial u}{\partial x} + v\frac{\partial u}{\partial y} = u_e\frac{du_e}{dx} + \frac{\partial u_e}{\partial t} + \frac{\mu_{hnf}}{\rho_{hnf}}\frac{\partial^2 u}{\partial y^2} + \frac{(\rho\beta)_{hnf}}{\rho_{hnf}}(T - T_\infty)g, \tag{2}$$

$$\frac{\partial T}{\partial t} + u\frac{\partial T}{\partial x} + v\frac{\partial T}{\partial y} = \frac{k_{hnf}}{(\rho C_p)_{hnf}}\frac{\partial^2 T}{\partial y^2}. \tag{3}$$

$$t \geq 0 : u = u_w + A_1 v\left(\frac{\partial u}{\partial y}\right), v = 0, T = T_w + B_1\left(\frac{\partial T}{\partial y}\right),$$
$$u \to u_e, T \to T_\infty, \text{ as } y \to \infty. \tag{4}$$

Here, T and g are the temperature and gravity acceleration, respectively. Next, $u_e = \frac{bx}{(1-ct)}$ with $b > 0$, $c \geq 0$ and $ct < 1$, $A_1 = A(1-ct)^{\frac{1}{2}}$ is the velocity slip factor, $T_w = T_\infty + \left[\frac{T_0 x}{L(1-ct)}^2\right]$ with L is characteristic of the plate, $T_0 > 0$ and $T_0 < 0$ defined the assisting flow and opposing flow, respectively. Further, $B_1 = B(1-ct)^{\frac{1}{2}}$ is the thermal slip factor, ρ_{hnf} and μ_{hnf} are the density and dynamic viscosity of working fluid, $(\rho C_p)_{hnf}$ is the hybrid nanofluids heat capacity and β_{hnf} is the thermal expansion coefficient. In addition, k is thermal conductivity and (ρC_p) is the heat capacity. The correlation coefficient of the hybrid nanofluids are given in Table 1 [19,20], while the physical characteristics are given in Table 2 [21].

Table 1
Fluid properties [19,20]

Properties	Alumina-Copper/Water
Thermal capacity	$(\rho C_p)_{hnf} = \phi_1(\rho C_p)_{s1} + \phi_2(\rho C_p)_{s2} + (1-\phi_{hnf})(\rho C_p)_f$
Thermal expansion	$\beta_{hnf} - (1-\phi_{hnf})\beta_f = \phi_1\beta_{s1} + \phi_2\beta_{s2}$
Thermal conductivity	$\frac{k_{hnf}}{k_f} = \left[\frac{\left(\frac{\phi_1 k_{s1} + \phi_2 k_{s2}}{\phi_{hnf}}\right) + 2k_f + 2(\phi_1 k_{s1} + \phi_2 k_{s2}) - 2\phi_{hnf} k_f}{\left(\frac{\phi_1 k_{s1} + \phi_2 k_{s2}}{\phi_{hnf}}\right) + 2k_f - (\phi_1 k_{s1} + \phi_2 k_{s2}) + \phi_{hnf} k_f}\right]$ where $\phi_{hnf} = \phi_1 + \phi_2$
Dynamic viscosity	$\mu_{hnf} = \frac{\mu_f}{(1-\phi_{hnf})^{2.5}}$
Density	$\rho_{hnf} = \phi_1\rho_{s1} + \phi_2\rho_{s2} + (1-\phi_{hnf})\rho_f$

Table 2
Fluid characteristic [21]

Characteristic	$\beta \times 10^{-5}(1/\mathrm{K})$	$\rho(\mathrm{kg/m^3})$	$k(\mathrm{W/mK})$	$C_p(\mathrm{J/kgK})$
H_2O	21	997.1	0.613	4179
Al_2O_3	0.85	3970	40	765
Cu	1.67	8933	400	385

Following that, we express the dimensionless variables listed below [12]:

$$\psi = \sqrt{\frac{a\nu_f}{1-ct}} x f(\eta), \theta(\eta) = \frac{T-T_\infty}{T_w - T_\infty}, \eta = y\sqrt{\frac{a}{\nu_f(1-ct)}}. \tag{5}$$

Using Eq. (5), Eq. (1) to Eq. (3) are modified as follows:

$$\frac{\frac{\mu_{hnf}}{\mu_f}}{\frac{\rho_{hnf}}{\rho_f}} f''' + ff'' - f'^2 + 1 + \varepsilon\left(1 - f' + \frac{1}{2}\eta f''\right) + \frac{\frac{(\rho\beta)_{hnf}}{(\rho\beta)_f}}{\frac{\rho_{hnf}}{\rho_f}}\lambda\theta = 0, \tag{6}$$

$$\frac{1}{Pr}\frac{\frac{k_{hnf}}{k_f}}{\frac{(\rho C_p)_{hnf}}{(\rho C_p)_f}}\theta'' + f\theta' - f'\theta - \varepsilon\left(2\theta + \frac{1}{2}\eta\theta'\right) = 0, \tag{7}$$

$$f(0) = 0, f'(0) = \delta + \gamma f''(0), \theta(0) = 1 + \vartheta\theta'(0),$$

$$f'(\eta) \to 1, \theta(\eta) \to 0 \text{ as } \eta \to \infty. \tag{8}$$

Here, $Pr = \frac{\nu_f}{\alpha_f}$ is the Prandtl number, $\varepsilon = \frac{c}{b}$ denotes as the unsteadiness parameter, and $\lambda = Gr_x/Re^2{}_x$ represents the mixed convection parameter where $\lambda > 0$ signifies the assisting flow and $\lambda < 0$ remarks the opposing flow. Next, $\gamma = A\sqrt{b\nu}$ is the velocity slip parameter and $\vartheta = B\sqrt{\frac{b}{\nu}}$ is the thermal slip parameter. The occurrence of velocity and thermal slip parameters will affect the velocity and temperature near the stretching/shrinking wall, respectively. This occurs as a result of the slip condition's ability to partially transmit the pulling of the stretching/shrinking wall to the working fluid. Meanwhile, $\delta = \frac{a}{b}$ is the ratio of stretching/shrinking parameter, while $\mathrm{Gr}_x = \frac{g\beta(T_w - T_\infty)x^3}{\nu_f^2}$ and $Re_x = \frac{u_e x}{\nu_f}$ are the local Grashof number and local Reynolds number, respectively. It is worth to mention that the Reynolds number is crucial for predicting the patterns of a fluid's behaviour. In this study, we focused on observing C_f as the skin friction coefficient and Nu_x which represents the local Nusselt number, denoted below:

$$C_f = \frac{\mu_{hnf}}{\rho_f u_e^2}\left(\frac{\partial u}{\partial y}\right)_{y=0}, \; Nu_x = \frac{x k_{hnf}}{k_f(T_w - T_\infty)}\left(-\frac{\partial T}{\partial y}\right)_{y=0}. \tag{9}$$

Using the listed expressions in Eqs. (5) and (9), we obtain:

$$Re_x^{\frac{1}{2}} C_f = \frac{\mu_{hnf}}{\mu_f} f''(0), \;\; Re_x^{-\frac{1}{2}} Nu_x = -\frac{k_{hnf}}{k_f}\theta'(0). \tag{10}$$

3. Stability Analysis

As there have been various solutions to the boundary value problem Eq. (6)−(7), an investigation of solution stability is conducted. Following the idea by Merkin [22], we introduced:

$$u = \frac{bx}{(1-ct)}\frac{\partial f}{\partial \eta}(\eta, \tau), v = -\sqrt{\frac{b\nu_f}{(1-ct)}} f(\eta, \tau), \theta(\eta, \tau) = \frac{T - T_\infty}{T_w - T_\infty}, \eta = \sqrt{\frac{b}{\nu_f(1-ct)}}, \tau = \frac{b}{(1-ct)}t. \tag{11}$$

Using Eq. (11), Eq. (6) to Eq. (7), as well as boundary conditions Eq. (8), are transformed and resulting in:

$$\frac{\frac{\mu_{hnf}}{\mu_f}}{\frac{\rho_{hnf}}{\rho_f}}\frac{\partial^3 f}{\partial \eta^3} + f\frac{\partial^2 f}{\partial \eta^2} + \varepsilon\left(1 - \frac{\partial f}{\partial \eta} - \frac{1}{2}\eta\frac{\partial^2 f}{\partial \eta^2}\right) + \frac{\frac{(\rho\beta)_{hnf}}{(\rho\beta)_f}}{\frac{\rho_{hnf}}{\rho_f}}\lambda\theta$$

$$-\left(\frac{\partial f}{\partial \eta}\right)^2 - (1 + \varepsilon\tau)\frac{\partial^2 f}{\partial \eta \partial \tau} + 1 = 0, \tag{12}$$

$$\frac{1}{Pr}\left(\frac{\frac{k_{hnf}}{k_f}}{\frac{(\rho c_p)_{hnf}}{(\rho c_p)_f}}\right)\frac{\partial^2 \theta}{\partial \eta^2} + f\frac{\partial \theta}{\partial \eta} - \frac{\partial f}{\partial \eta}\theta - \varepsilon\left(2\theta + \frac{\eta}{2}\right)\frac{\partial \theta}{\partial \eta} - (1 + \varepsilon\tau)\frac{\partial \theta}{\partial \tau} = 0, \tag{13}$$

$$f(0,\tau)=0,\quad \frac{\partial f}{\partial \eta}(0,\tau)=\delta+\gamma\frac{\partial^2 f}{\partial \eta^2}(0,\tau),\ \theta(0,\tau)=1+\vartheta\theta'(0,\tau),$$

$$\frac{\partial f}{\partial \eta}(\eta,0)\to 1,\quad \theta(\eta,0)\to 0,\text{as}\ \eta\to\infty. \tag{14}$$

After that, referring to the work done in Ref. [23], we have:

$$f(\eta,\tau)=f_0(\eta)+e^{-\xi\tau}F(\eta),\quad \theta(\eta,\tau)=\theta_0(\eta)+e^{-\xi\tau}G(\eta), \tag{15}$$

where, $F(\eta)$ and $G(\eta)$ are relatively small to $f_0(\eta)$ and $\theta_0(\eta)$ whilst ξ is the unidentified eigenvalue. Substituting Eq. (15) into Eq. (12) to Eq. (13), thus:

$$\frac{\frac{\mu_{hnf}}{\mu_f}}{\frac{\rho_{hnf}}{\rho_f}}\frac{\partial^3 F}{\partial \eta^3}+f_0\frac{\partial^2 F}{\partial \eta^2}+\xi\frac{\partial F}{\partial \eta}-2\frac{\partial^2 f_0{}'}{\partial \eta^2}\frac{\partial F}{\partial \eta}+\frac{\partial^2 f_0{}''}{\partial \eta^2}F+1-\varepsilon\left(\frac{\partial F}{\partial \eta}+\frac{1}{2}\eta\frac{\partial^2 F}{\partial \eta^2}\right)+\frac{\frac{(\rho\beta)_{hnf}}{(\rho\beta)_f}}{\frac{\rho_{hnf}}{\rho_f}}\lambda G=0, \tag{16}$$

$$\frac{1}{Pr}\frac{\frac{k_{hnf}}{k_f}}{\frac{(\rho C_p)_{hnf}}{(\rho C_p)_f}}\frac{\partial^2 G}{\partial \eta^2}+f_0\frac{\partial G}{\partial \eta}+F\frac{\partial \theta_0}{\partial \eta}-\left(G\frac{\partial f_0}{\partial \eta}+\theta_0\frac{\partial F}{\partial \eta}\right)-\varepsilon\left(2G+\frac{\eta}{2}\frac{\partial G}{\partial \eta}\right)+\xi G=0, \tag{17}$$

$$F(0,\tau)=0,\quad \frac{\partial F}{\partial \eta}(0,\tau)=\gamma\frac{\partial^2 F}{\partial \eta^2}(0,\tau),G(0,\tau)=\vartheta\frac{\partial G}{\partial \eta}(0,\tau),$$

$$\frac{\partial F}{\partial \eta}(\eta,\tau)\to 0,\quad G(\eta,\tau)\to 0,\ \text{as}\quad \eta\to\infty \tag{18}$$

Now we set $\tau\to 0$ and placing the linearisation process into practise, thus

$$\frac{\frac{\mu_{hnf}}{\mu_f}}{\frac{\rho_{hnf}}{\rho_f}}F'''+f_0F''+Ff_0-2f_0{}'F''+1-\varepsilon\left(F'+\frac{1}{2}\eta F''\right)+\frac{\frac{(\rho\beta)_{hnf}}{(\rho\beta)_f}}{\frac{\rho_{hnf}}{\rho_f}}\lambda G+\xi F'=0, \tag{19}$$

$$\frac{1}{Pr}\frac{\frac{k_{hnf}}{k_f}}{\frac{(\rho C_p)_{hnf}}{(\rho C_p)_f}}G''+\left(f_0-\varepsilon\frac{\eta}{2}\right)G'-\left(f_0{}'+2\varepsilon\right)G+F_0\theta'-F'\theta_0+\xi G=0, \tag{20}$$

$$F(0)=0,\quad F'(0)=\gamma F''(0),\quad G(0)=\vartheta G'(0),$$

$$F'(\eta)\to 0,\quad G(\eta)\to 0. \tag{21}$$

According to Ref. [24], when one of the boundary conditions is eliminated, the potential eigenvalues become obtainable. Hence, in this study, $F''(0)=1$ is implemented by replacing the value of $F'(\eta)\to 0$ as $\eta\to\infty$ in boundary conditions Eq. (21) as ξ_1 is established.

4. Results and Discussion

The bvp4c solver in MATLAB software was used to numerically solve Eq. (6) and Eq. (7) with respect to boundary conditions in Eq. (8). The bvp4c is a finite difference code that implements the three-stage Lobatto IIIa formula. This formula uses collocation, and the collocation polynomial offers a C^1-continuous solution that is consistently fourth-order accurate in the interval of integration. The reliability of the current results is confirmed by comparing the numerical data with Dinarvand and Hosseini [25], as reported in Table 3. Since the current results are completely consistent, we claim the acquired findings are valid and dependable. Next, the influence of specific physical characteristics is then investigated, and the results are presented in graphical form. It is noticed that there exist multiple solutions in this study, therefore a stability solution is required. The idea of stability derives from a laminar flow which is slightly disturbed. Once the laminar flow returns to its original state, the flow is considered stable; however, if the disturbance rises and changes the laminar state into a different state, the flow is defined unstable. In a normal situation, the first solution is usually reliable because it satisfies the far-field boundary condition. The smallest eigenvalue denotes as ξ_1 shows the solutions properties in the stability analysis technique. The flow is considered stable if ξ_1 is positive because it meets the stabilising feature. On the other hand, the flow is denoted as unstable when ξ_1 is negative. In this study, the first solutions with the positive eigenvalues distract the growth of the disturbance in the solutions at some range of the mixed convection parameter in the opposing flow $(\lambda < 0)$, hence returning the flow to its original state. Thus, we can conclude that the first solution is stable and reliable, whereas the second solution is not, as seen in Table 4.

Table 3
Variations of $f''(0)$ and $-\theta'(0)$ with assorted Pr as $\phi_1 = \phi_2 = \varepsilon = \gamma = \delta = \vartheta = 0$, and $\lambda = 1.0$

Pr	$f''(0)$		$-\theta'(0)$	
	Dinarvand and Hosseini [25]	Current result	Dinarvand and Hosseini [25]	Current result
0.7	1.7063	1.706323	0.7641	0.764063
1.0	1.6754	1.675437	0.8708	0.870779
7.0	1.5178	1.517913	1.7225	1.722382
10.0	14927	1.492839	1.9444	1.944617
20.0	1.4482	1.448483	2.4573	2.457590
40.0	1.4104	1.410058	3.1014	3.101093
50.0	1.3986	1.398930	3.3418	3.341458

Table 4
Variations of ξ_1 with assorted λ

λ	First sol.	Second sol.
-0.01	0.7054	-0.8912
-0.02	0.4821	-0.5426
-0.03	0.2519	-0.3674
-0.04	0.0037	-0.0048
-0.05	0.0003	-0.0011

*Note: sol. = solution

The characteristics of $f''(0)$ which represents the skin friction coefficient in pure water $(\phi_1 = \phi_2 = 0.00)$, nanofluids $(\phi_1 = 0.00, \phi_2 = 0.01)$ and hybrid nanofluids $(\phi_1 = \phi_2 = 0.05)$ are available in Figure 2(a), while the heat transfer rate $-\theta'(0)$ is portrayed in Figure 2(b). It is observed

that the similarity solutions for viscous flow $(\phi_1 = \phi_2 = 0.00)$ are available when $\lambda \geq \lambda_c = -0.0394$. The range of solution becomes wider when the nanoparticle volume fraction is added where $\lambda \geq \lambda_c = -0.0422$ and $\lambda \geq \lambda_c = -0.0481$ denote the Al_2O_3/H_2O nanofluids and Al_2O_3-Cu/H_2O hybrid nanofluids, respectively. Figure 2(a) indicates that the growth of ϕ_2 enhances $f''(0)$; thus, this signifies $f''(0)$ of Al_2O_3-Cu/H_2O is more significant than Al_2O_3/H_2O and water when 1% and 5% of ϕ_2 (Cu) volume concentration is presented. The Al_2O_3-Cu/H_2O characteristics are portrayed in Figure 3(a) concerning $f''(0)$ toward the stretching/shrinking vertical plate λ as ε varied. Figure 3(a) shows that as ε improved, $f''(0)$ increases in the first solution. Figure 3(b) demonstrates an increasing pattern of $-\theta'(0)$ when ϕ_2 improves in the first solution. As a result, thermal performance quality has improved as the viscous flow transforms into Al_2O_3/H_2O nanofluids and Al_2O_3-Cu/H_2O hybrid nanofluids past the shrinking vertical plate. Also, Figure 3(b) observes that $-\theta'(0)$ is improved when ε escalates in the first solution. It should be noted that a rise in ϕ_2 and ε has broadened the range of solutions as seen in Figure 2 and Figure 3, hence permitted for a delay in the boundary layer separation process.

The profile of velocity $f'(\eta)$, which is presented in Figure 4(a), demonstrates that the momentum boundary layer depth improved as ε increased. This phenomenon boosts the Al_2O_3-Cu/H_2O density and eventually increases the velocity gradient hence improving $f'(\eta)$. The temperature profiles $\theta(\eta)$ in Figure 4(b) back up the trend seen in Figure 3(b), which shows how the temperature of changes as ε increases. The deterioration in Al_2O_3-Cu/H_2O temperature declines the thermal transmission and gradually upsurges the convective heat transfer rate. Figure 5(a), Figure (b) and Figure 6(a), Figure 6(b) present another sample of $f'(\eta)$ and $\theta(\eta)$ for certain range of γ and ϑ parameter, respectively. Based on our findings, all profiles asymptotically satisfy the free stream conditions (8), which then authorises the validity of the numerical. The decreasing trend of the first solution results in $f'(\eta)$ and $\theta(\eta)$ is figured out with the rising values of γ in Figure 5(a) and Figure 5(b), respectively. Meanwhile, as ϑ boosts up, the first solution in $f'(\eta)$ and $\theta(\eta)$ is enlarged as displayed in Figure 6(a) and Figure 6(b). However, the second solution is decreases as the thermal slip parameter improves in both velocity and temperature distribution profiles.

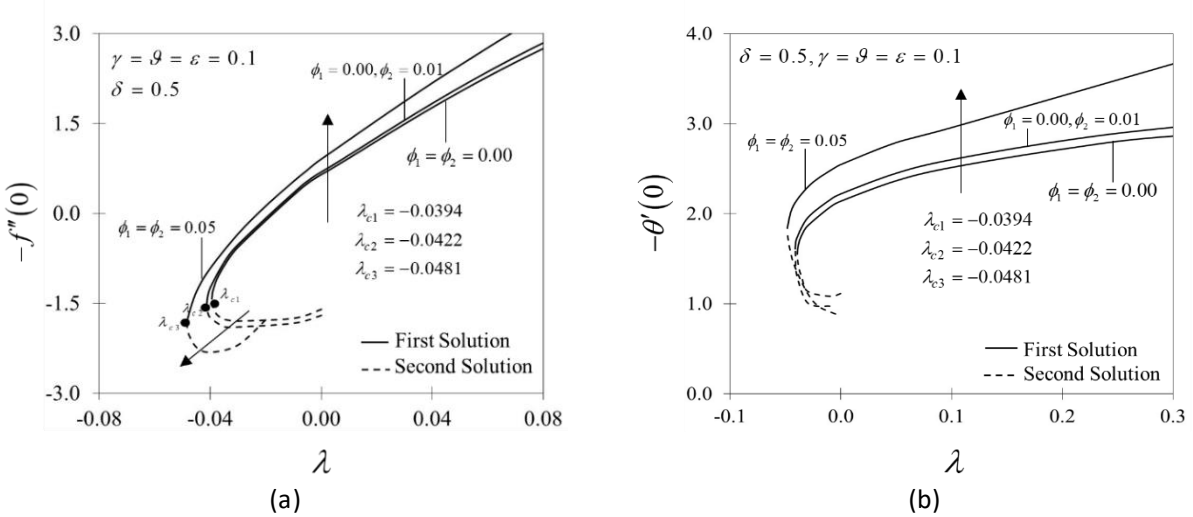

Fig. 2. Different values of ϕ_1 and ϕ_2 with λ (a) reduced skin friction coefficient (b) reduced heat transfer coefficient

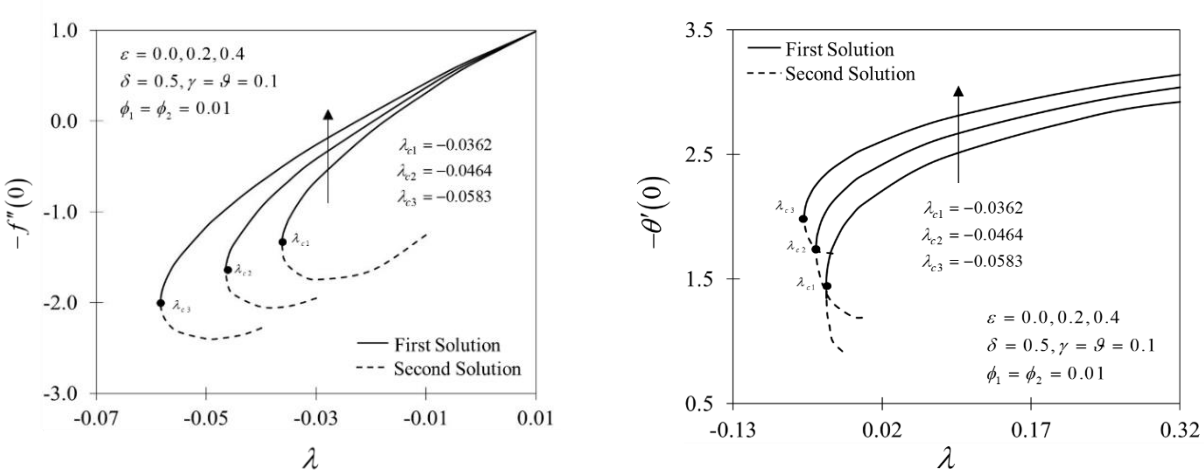

(a) (b)

Fig. 3. Different values of ε with λ (a) reduced skin friction coefficient (b) reduced heat transfer coefficient

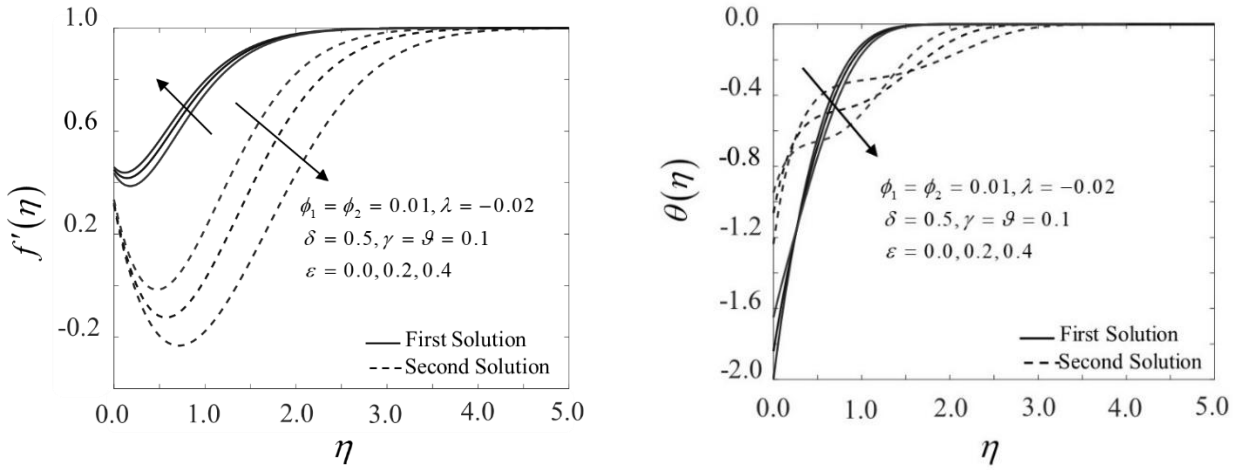

(a) (b)

Fig. 4. Different values of ε with η (a) velocity profile (b) temperature profile

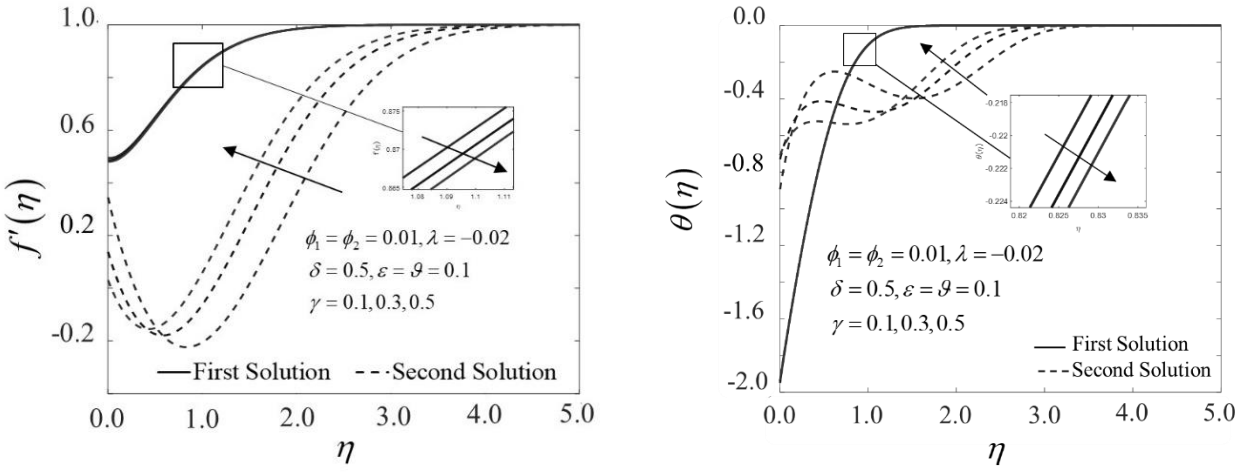

(a) (b)

Fig. 5. Different values of γ with η (a) velocity profile (b) temperature profile

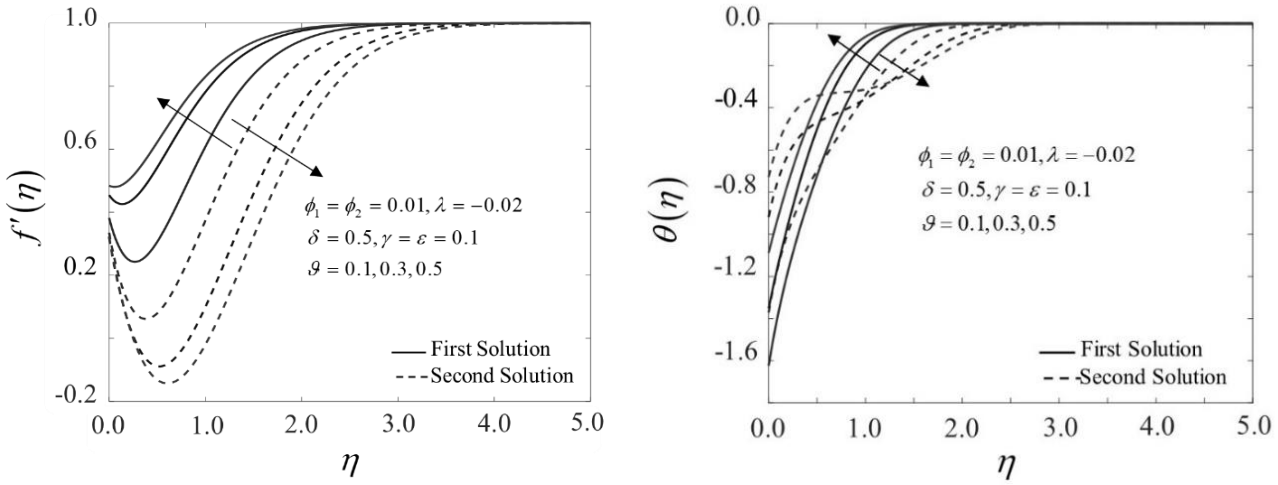

Fig. 6. Different values of ϑ with η (a) velocity profile (b) temperature profile

5. Conclusions

The current work verified a numerical evaluation of the unsteady mixed convection stagnation point of Al_2O_3-Cu/H_2O hybrid nanofluid towards a stretching/shrinking vertical plate. According to our observations, the presence of the first and second solution is demonstrated for a wide range of control parameters throughout the Al_2O_3-Cu/H_2O combination, and evidently, the thermal efficiency can be improved by increasing the nanoparticle volume fraction concentration. This means that the hybrid nanofluids have a higher thermal conductivity than the nanofluids and traditional fluids. Also, the increment of the unsteadiness parameter stimulates the thermal performance enhancement in the Al_2O_3-Cu/H_2O. The consistency of the first solution is ensured by the analysis of solution stability.

Acknowledgement

This research is supported by TAP-K007136 from Universiti Kebangsaan Malaysia, and the Universiti Teknikal Malaysia Melaka is gratefully acknowledged.

References

[1] Huminic, Gabriela, and Angel Huminic. "Hybrid nanofluids for heat transfer applications–a state-of-the-art review." *International Journal of Heat and Mass Transfer* 125 (2018): 82-103. https://doi.org/10.1016/j.ijheatmasstransfer.2018.04.059

[2] Sidik, Nor Azwadi Che, Isa Muhammad Adamu, Muhammad Mahmud Jamil, G. H. R. Kefayati, Rizalman Mamat, and G. Najafi. "Recent progress on hybrid nanofluids in heat transfer applications: a comprehensive review." *International Communications in Heat and Mass Transfer* 78 (2016): 68-79. https://doi.org/10.1016/j.icheatmasstransfer.2016.08.019

[3] Suresh, S., K. P. Venkitaraj, and P. Selvakumar. "Synthesis, characterisation of Al2O3-Cu nano composite powder and water based nanofluids." In *Advanced Materials Research*, vol. 328, pp. 1560-1567. Trans Tech Publications Ltd, 2011. https://doi.org/10.4028/www.scientific.net/AMR.328-330.1560

[4] Ahmed, Sohail, and Hang Xu. "Mixed convection in gravity-driven thin nano-liquid film flow with homogeneous–heterogeneous reactions." *Physics of Fluids* 32, no. 2 (2020): 023604. https://doi.org/10.1063/1.5140366

[5] Ahmed, Sohail, Hang Xu, and Qiang Sun. "Stagnation flow of a SWCNT nanofluid towards a plane surface with heterogeneous-homogeneous reactions." *Mathematical Problems in Engineering* 2020 (2020): 1-12. https://doi.org/10.1155/2020/3265143

[6] Ahmed, Sohail, Hang Xu, Yue Zhou, and Qiang Yu. "Modelling convective transport of hybrid nanofluid in a lid driven square cavity with consideration of Brownian diffusion and thermophoresis." *International Communications in Heat and Mass Transfer* 137 (2022): 106226. https://doi.org/10.1016/j.icheatmasstransfer.2022.106226

[7] Ahmed, Sohail, and Hang Xu. "Forced convection with unsteady pulsating flow of a hybrid nanofluid in a microchannel in the presence of EDL, magnetic and thermal radiation effects." *International Communications in Heat and Mass Transfer* 120 (2021): 105042. https://doi.org/10.1016/j.icheatmasstransfer.2020.105042

[8] Khan, Naseer M., Yu-Ming Chu, Muhammad Ijaz Khan, Seifedine Kadry, and Sumaira Qayyum. "Modeling and dual solutions for magnetized mixed convective stagnation point flow of upper convected Maxwell fluid model with second-order velocity slip." *Mathematical Methods in the Applied Sciences* (2020). https://doi.org/10.1002/mma.6824

[9] Abbas, Syed Zaheer, M. Waqas, Adel Thaljaoui, M. Zubair, Anis Riahi, Y. M. Chu, and Waqar Azeem Khan. "Modeling and analysis of unsteady second-grade nanofluid flow subject to mixed convection and thermal radiation." *Soft Computing* (2022): 1-10. https://doi.org/10.1007/s00500-021-06575-7

[10] Chu, Yu-Ming, Nargis Khan, M. Ijaz Khan, Kamel Al-Khaled, Nasreen Abbas, Sami Ullah Khan, Muhammad Sadiq Hashmi, Sumaira Qayyum, and S. Kadry. "Thermophoresis particle deposition analysis for nonlinear thermally developed flow of Magneto-Walter's B nanofluid with buoyancy forces." *Alexandria Engineering Journal* 60, no. 1 (2021): 1851-1860. https://doi.org/10.1016/j.aej.2020.11.033

[11] Chu, Yu-Ming, M. Israr Ur Rehman, M. Ijaz Khan, S. Nadeem, Seifedine Kadry, Zahra Abdelmalek, and Nadeem Abbas. "Transportation of heat and mass transport in hydromagnetic stagnation point flow of Carreau nanomaterial: Dual simulations through Runge-Kutta Fehlberg technique." *International Communications in Heat and Mass Transfer* 118 (2020): 104858. https://doi.org/10.1016/j.icheatmasstransfer.2020.104858

[12] Jamaludin, Anuar, Roslinda Nazar, and Ioan Pop. "Mixed convection stagnation-point flow of a nanofluid past a permeable stretching/shrinking sheet in the presence of thermal radiation and heat source/sink." *Energies* 12, no. 5 (2019): 788. https://doi.org/10.3390/en12050788

[13] Devi, CD Surma, H. S. Takhar, and G. Nath. "Unsteady mixed convection flow in stagnation region adjacent to a vertical surface." *Wärme-und Stoffübertragung* 26, no. 2 (1991): 71-79. https://doi.org/10.1007/BF01590239

[14] Noor, Amin, Roslinda Nazar, Kohilavani Naganthran, and Ioan Pop. "Unsteady mixed convection flow at a three-dimensional stagnation point." *International Journal of Numerical Methods for Heat & Fluid Flow* 31, no. 1 (2021): 236-250. https://doi.org/10.1108/HFF-03-2020-0138

[15] Kamal, Mohamad Hidayad Ahmad, Anati Ali, Lim Yeou Jiann, Noraihan Afiqah Rawi, and Sharidan Shafie. "Stagnation point flow of a hybrid nanofluid under the gravity modulation effect." *Journal of Advanced Research in Fluid Mechanics and Thermal Sciences* 92, no. 2 (2022): 157-170. https://doi.org/10.37934/arfmts.92.2.157170

[16] Ali, I. R., Ammar I. Alsabery, Norhaliza Abu Bakar, and Rozaini Roslan. "Mixed Convection in a Lid-Driven Horizontal Rectangular Cavity Filled with Hybrid Nanofluid by Finite Volume Method." *Journal of Advanced Research in Fluid Mechanics and Thermal Sciences* 93, no. 1 (2022): 110-122. https://doi.org/10.37934/arfmts.93.1.110122

[17] Waini, Iskandar, Anuar Ishak, and Ioan Pop. "MHD Glauert flow of a hybrid nanofluid with heat transfer." *Joumal of Advanced Research in Fluid Mechanics and Thermal Sciences* 86, no. 2 (2021): 91-100. https://doi.org/10.37934/arfmts.86.2.91100

[18] Idris, Muhammad Syafiq, Irnie Azlin Zakaria, and Wan Azmi Wan Hamzah. "Heat transfer and pressure drop of water based hybrid Al2O3: SiO2 nanofluids in cooling plate of PEMFC." *Journal of Advanced Research in Numerical Heat Transfer* 4, no. 1 (2021): 1-13.

[19] Ghalambaz, Mohammad, Natalia C. Roşca, Alin V. Roşca, and Ioan Pop. "Mixed convection and stability analysis of stagnation-point boundary layer flow and heat transfer of hybrid nanofluids over a vertical plate." *International Journal of Numerical Methods for Heat & Fluid Flow* 30, no. 7 (2020): 3737-3754. https://doi.org/10.1108/HFF-08-2019-0661

[20] Takabi, Behrouz, and Saeed Salehi. "Augmentation of the heat transfer performance of a sinusoidal corrugated enclosure by employing hybrid nanofluid." *Advances in Mechanical Engineering* 6 (2014): 147059. https://doi.org/10.1155/2014/147059

[21] Oztop, Hakan F., and Eiyad Abu-Nada. "Numerical study of natural convection in partially heated rectangular enclosures filled with nanofluids." *International journal of heat and fluid flow* 29, no. 5 (2008): 1326-1336. https://doi.org/10.1016/j.ijheatfluidflow.2008.04.009

[22] Merkin, J. H. "On dual solutions occurring in mixed convection in a porous medium." *Journal of engineering Mathematics* 20, no. 2 (1986): 171-179. https://doi.org/10.1007/BF00042775

[23] Weidman, P. D., D. G. Kubitschek, and A. M. J. Davis. "The effect of transpiration on self-similar boundary layer flow over moving surfaces." *International journal of engineering science* 44, no. 11-12 (2006): 730-737. https://doi.org/10.1016/j.ijengsci.2006.04.005

[24] Harris, S. D., D. B. Ingham, and I. Pop. "Mixed convection boundary-layer flow near the stagnation point on a vertical surface in a porous medium: Brinkman model with slip." *Transport in Porous Media* 77 (2009): 267-285. https://doi.org/10.1007/s11242-008-9309-6

[25] Dinarvand, Saeed, Reza Hosseini, and Ioan Pop. "Homotopy analysis method for unsteady mixed convective stagnation-point flow of a nanofluid using Tiwari-Das nanofluid model." *International Journal of Numerical Methods for Heat & Fluid Flow* 26, no. 1 (2016): 40-62. https://doi.org/10.1108/HFF-12-2014-0387